



HAL
open science

Macroscopic fluctuations of a driven tracer in the symmetric exclusion process

Rahul Dandekar, Kirone Mallick

► **To cite this version:**

Rahul Dandekar, Kirone Mallick. Macroscopic fluctuations of a driven tracer in the symmetric exclusion process. *Journal of Physics A: Mathematical and Theoretical*, 2022, 55 (43), pp.435001. 10.1088/1751-8121/ac9766 . cea-04478332

HAL Id: cea-04478332

<https://cea.hal.science/cea-04478332>

Submitted on 26 Feb 2024

HAL is a multi-disciplinary open access archive for the deposit and dissemination of scientific research documents, whether they are published or not. The documents may come from teaching and research institutions in France or abroad, or from public or private research centers.

L'archive ouverte pluridisciplinaire **HAL**, est destinée au dépôt et à la diffusion de documents scientifiques de niveau recherche, publiés ou non, émanant des établissements d'enseignement et de recherche français ou étrangers, des laboratoires publics ou privés.

Macroscopic fluctuations of a driven tracer in the symmetric exclusion process

Rahul Dandekar and Kirone Mallick

Institut de Physique Theorique, CEA, CNRS, Universite Paris-Saclay, F-91191
Gif-sur-Yvette cedex, France

Abstract. The dynamics of an asymmetric tracer in the symmetric simple exclusion process is mapped, in the continuous scaling limit, to the local current through the origin in the zero-range process (ZRP) with a biased bond. This allows us to study the hydrodynamics of the SEP with an asymmetric tracer with a step initial condition, leading to the average displacement as a function of the bias and the densities on both sides. We then derive the cumulant generating function of the process in the high-density limit, by using the Macroscopic Fluctuation Theory and obtain agreement with the microscopic results of Poncet et al (2021). For more general initial conditions, we show that the tracer variance in the high-density limit depends only on the generalized susceptibility in the initial condition.

1. Introduction

Stochastic lattice gases of interacting particles are invaluable models to explore the dynamics of many-body systems: powerful theoretical tools have been developed to study them in the physics and the mathematical literature (some general references are [1, 2, 3, 4, 5]). Many of these processes appeared in biophysics to represent molecular motors or biopolymerization on nucleic acid templates [6, 7]. Among numerous models, the one-dimensional simple exclusion process – in which particles perform random walks subject to the constraint that a site can be occupied by at most one particle at a given time – has acquired a paradigmatic status, thanks to its rich combinatorial structure that has led to many exact analytical results [8, 9]. In particular, the macroscopic hydrodynamics of the simple exclusion process is by now well understood [10, 1] and the analysis of the microscopic process allows one to probe fluctuations beyond the average hydrodynamic behavior. Indeed, noise at the lattice size scale can affect the coarse-grained evolution of the system and generate rare events (or large deviations) with drastic impact [11, 12, 9].

Another manner to explore the interplay between the microscopic and macroscopic scales is to consider a probe particle (also called a tracer) and follow its motion in the surrounding fluid of particles. If the tracer follows the same dynamical rules as the other particles, it behaves as a passive scalar and does not affect the hydrodynamics. However, if the probe behaves in a different manner (it is sensitive to an external drive,

or it is *active* in some way), then the overall collective dynamics can be altered. This is precisely the type of effect we wish to investigate in the present work.

We shall consider the one-dimensional symmetric simple exclusion process (SEP) on the infinite one-dimensional lattice with a single biased tracer (or tagged particle). This biased tracer hops with rate r_+ to its right neighbor and r_- to its left, while all other particles hop at rate 1 in either direction. All particles, including the tracer, are subject to the exclusion condition and their order remains unchanged: this is a single file-dynamics. It is known [13, 14, 15, 16] that the average displacement of the biased tracer in an infinite system grows, for large times, as

$$\langle X_t \rangle = \sqrt{2ct} \quad (1)$$

where X_t is the displacement of the tracer at time t , and c is a number that depends on the initial density profile and on the tracer bias through the ratio $\frac{r_+}{r_+ + r_-}$. If the tracer particle is symmetric and has the same dynamics as all other particles, the variance of the tracer displacement for large times grows as

$$\langle X_t^2 \rangle - \langle X_t \rangle^2 = \sigma_{\text{ic}} \sqrt{t} \quad (2)$$

where σ_{ic} is a constant that depends on the initial densities on either side of the tracer and on the initial set-up of the system [17, 18, 19, 20, 21, 22, 23]. More generally, for reflecting Brownian motions [22, 24] and for the SEP [25], it is possible to calculate all the cumulants of the position of an unbiased tracer, that all grow with time as \sqrt{t} .

For a biased tracer, the behavior of the variance is not known in most cases even for the SEP. In the high-density limit, $\rho \rightarrow 1$, it has been shown that equation (2) is valid for the driven tracer as well, and the coefficient σ_{ic} can be computed microscopically [15, 26]. In fact, in the high-density limit, the full cumulant generating function of the tracer position can be calculated from microscopic dynamics [27]. However, many questions remain unanswered and a more general framework for studying the driven tracer would be useful.

In the present work, we study the asymmetric tracer in the framework of Macroscopic Fluctuation Theory (MFT), by extending the hydrodynamic approach to asymmetric tracers developed by Landim, Olla and Volchan [28, 29]. For symmetric single-file systems, the MFT [30, 9] allows one to derive statistical results for quantities like the current fluctuations [31] and the tracer position [23] in terms of the diffusivity and conductivity coefficients of the hydrodynamic description. However, the presence of the biased tracer generates a moving boundary condition at the macroscopic level. A suitable way to derive this condition is to use a mapping between single-file systems and mass transfer processes. In particular, the SEP in 1D is mapped to the 1D Zero-range process (ZRP) [32, 33] and the biased particle in the SEP becomes a biased bond in the ZRP. It can be shown (see section 3) that, for any density, the dynamics depends on r_- and r_+ only through the parameter $\frac{r_+}{r_+ + r_-}$. In the high-density limit of the SEP, the MFT equations can be solved and the full cumulant generating function of the tracer

position can be calculated. Our results agree with the microscopic derivations in [15, 26]. Recently, the dependence of the variance of the tracer position on the initial state has been investigated in a broader class of initial states and shown to depend on the initial state only through a specific quantity, the generalized compressibility [34]. The MFT allows us to study these more general initial states and we show that

$$\langle X_t^2 \rangle - \langle X_t \rangle^2 = (\alpha_{\text{ic}} \sigma_{\text{annealed}} + (1 - \alpha_{\text{ic}}) \sigma_{\text{quenched}}) \sqrt{t} \quad (3)$$

where α_{ic} is the generalized susceptibility of the initial ensemble, and σ_{annealed} and σ_{quenched} are the coefficients of the tracer variance for quenched (deterministic) and annealed (fluctuating) initial conditions respectively.

The outline of this work is as follows. In Section 2, we describe the general mapping between single-file systems and a dual mass-transfer process at the hydrodynamic level, that generalizes a known microscopic mapping between the SEP and the ZRP. In Section 3, we first describe the hydrodynamic approach to calculating the average displacement of a driven tracer in the SEP for any density and then, we derive the complete MFT boundary conditions at the tracer using the mapping to a mass transfer process. In section 4, we solve the case of the SEP in the high-density limit, $\rho \rightarrow 1$ and calculate the full cumulant generating function for the tracer position using the MFT, recovering the microscopic results of [15, 26]. We also calculate the dependence of the variance on the initial condition and show that it depends only on the generalized compressibility. Section 5 is devoted to concluding remarks.

2. Single-file and mass-transfer processes

In a single-file process on a one-dimensional lattice the particle order is conserved by the dynamical rules, because overtaking is forbidden. The Symmetric Simple Exclusion Process (SEP) is an archetypical single-file model and its well-known mapping to the Zero Range Process (ZRP) [32, 33] goes as follows (see Fig. 1):

- (i) Label the SEP particles at the initial time ($t = 0$), starting from the origin, with $i = 0$ being the particle with the smallest non-negative position, $i = 1$ being the next particle to the right, and so on. Call z_i the number of empty sites between particles i and $i + 1$.
- (ii) Consider a ZRP with masses z_i on site i and rate $r = 1$ of mass transfer from each occupied site to each of its neighbors, irrespective of the mass z on the site.
- (iii) A mass transfer to the right results in z_i decreasing by one, and z_{i+1} increasing by one. Thus, in the SEP, it corresponds to particle $i + 1$ hopping to the left. Thus, the mapping between the SEP and ZRP dynamics is that the current (or mass transfer) in the ZRP along the bond $[i - 1, i]$ to the left (right) corresponds to the particle with label i in the SEP hopping to the right (left).

The particle with label $i = 0$, having the smallest non-negative initial position will be hereafter called the *tracer*. Its position with time will be denoted as $X(t)$. In the

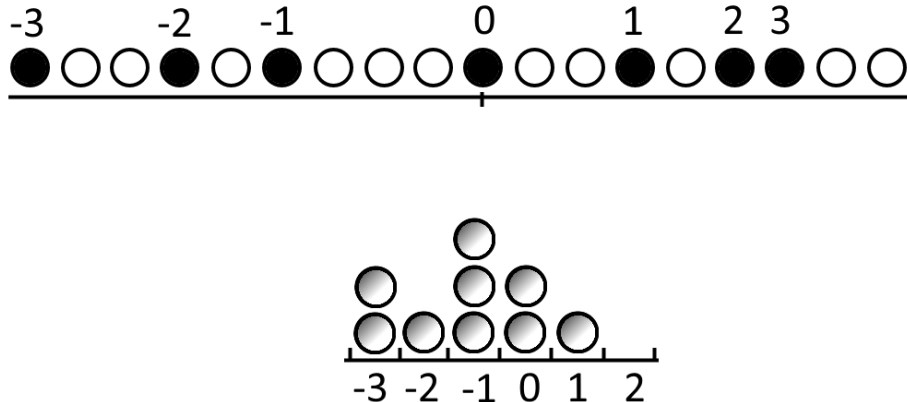


Figure 1. A configuration in the SEP (left) and its corresponding ZRP configuration (right). The particle with label i in SEP becomes the site i in ZRP and the number of marbles over site i in ZRP corresponds to the number of holes between the successive particles i and $i + 1$ in SEP.

ZRP language, the tracer is mapped to the site 0 and tracer movement to mass transfer along the bond $[-1, 0]$.

2.1. Mapping a single-file to a mass-transfer process

In this subsection we present a general mapping of the continuum limit of an arbitrary single-file diffusion system to a mass-transfer process, generalizing the mapping of the previous section. Our aim is to relate precisely the statistical fluctuations of these two types of models. From now on, observables that refer to a single-file process will be written with a subscript s and the spatial coordinate in the single-file process is denoted by x . Quantities related to a mass-transfer model have a subscript m and the spatial coordinate is denoted by z . Hence, $\rho_s(x)$ and $\rho_m(z)$ represent the local density in the single-file process and in the mass-transfer process, respectively.

Using the same underlying idea as that the one explained in the previous subsection, the transformation laws for the coordinates and the densities can be written as follows:

$$z = \int_{X(t)}^x \rho_s(u, t) du \quad (4)$$

$$\int_0^z \rho_m(u, t) du = \int_{X(t)}^x (1 - \rho_s(u, t)) du \quad (5)$$

The first equation says that a distance z in the mass-transfer process corresponds to the total number of particles between the tracer (located at $X(t)$) and the position x of the z^{th} particle in the single-file. The second equation expresses the fact that the total mass between 0 and z in the mass-transfer process is equal to the total number of holes between $X(t)$ and x in the single-file. Finally, the position of the tracer $X(t)$ is given

by *minus* the mass-transfer through the origin

$$X(t) = -J(t) = \int_0^\infty (\rho_m(u, 0) - \rho_m(u, t)) du \quad (6)$$

Equations (4), (5) and (6) define a complete macroscopic one-to-one mapping between the single-file and the mass-transfer processes. In particular, differentiating eqns. (4) and (5) with respect to x , we deduce that the local densities in the two processes are related through

$$\rho_s(x, t) = \frac{1}{\rho_m(z, t) + 1} \quad (7)$$

The transformation (4) and (5) can be inverted as

$$x(z, t) = X(t) + z + \int_0^z \rho_m(u, t) du, \quad (8)$$

and hence

$$\frac{dx}{dz} = 1 + \rho_m(z, t) = \frac{1}{\rho_s(x, t)}. \quad (9)$$

We now relate the diffusivities of the two models to each other. Consider the current in a coarse-grained single-file system in the presence of a uniform density gradient,

$$j_s = -D_s(\rho_s) \frac{d\rho_s}{dx}$$

This would also cause a current in the mass transfer process. Since transfer across a bond in the mass transfer process corresponds to the motion of a particle (in the opposite direction) in the single-file system, we have, for the current in the mass transfer process,

$$j_s = -\rho_s j_m, \text{ that is, } j_m = -\frac{j_s}{\rho_s}. \quad (10)$$

Using (7) and (8), we obtain (note that the density gradient is of opposite sign after the transformation)

$$j_m = -\frac{1}{(1 + \rho_m)^2} D_s \left(\frac{1}{1 + \rho_m} \right) \frac{d\rho_m}{dz} = -D_m(\rho_m) \frac{d\rho_m}{dz}$$

Hence, the diffusivity for the mass transfer process is related to the diffusivity of the single-file system through the relation

$$D_m(\rho_m) = \frac{1}{(1 + \rho_m)^2} D_s \left(\frac{1}{1 + \rho_m} \right), \text{ or } D_s(\rho_s) = \frac{1}{\rho_s^2} D_m \left(\frac{1}{\rho_s} - 1 \right) \quad (11)$$

2.2. MFT equations and the cumulant generating function for the current

The Macroscopic Fluctuation Theory is defined in terms of two hydrodynamic coefficients, the diffusivity $D(\rho)$ and the conductivity $\sigma(\rho)$. The Macroscopic

Fluctuating Theory equations for a stochastic process with diffusivity D and conductivity σ are given, in the bulk, by

$$\partial_t q = \partial_x(D(q)\partial_x q) - \partial_x(\sigma(q)\partial_x p) \quad (12a)$$

$$\partial_t p = -D(q)\partial_{xx} p - \sigma'(q)(\partial_x p)^2 \quad (12b)$$

We will consider the calculation of the cumulant generating function for the current across the origin in time T , $J(T)$

$$\mu(\lambda) = \log \langle e^{\lambda J(T)} \rangle \quad (13)$$

where the angular brackets denote the average over all paths, weighted by the path action S . $\mu(\lambda)$ can be calculated from the current through the origin in the MFT. (See also [35]). Let the notation $J[\mathcal{P}]$ denote the value of J calculated along a particular trajectory \mathcal{P} of the system. Differentiating, we have

$$\mu'(\lambda) = \frac{\langle J e^{\lambda J} \rangle}{\langle e^{\lambda J} \rangle} = \langle J \rangle_\lambda$$

where the final average is over the tilted action, $S + \lambda J$.

Let us assume that, in the hydrodynamic limit, the tilted action is dominated by a single trajectory, $\mathcal{P}_S(\lambda)$, the saddle-point trajectory. Then,

$$\mu'(\lambda) = J[\mathcal{P}_S(\lambda)] = J_{MFT} \quad (14)$$

since the MFT equations provide the saddle-point solution to the tilted action. One can thus calculate the CGF from the current in the MFT solution, along with the condition that $\mu(\lambda = 0) = 0$.

The MFT equations (12a) and (12b) are supplemented by boundary conditions, which depend on the quantity being calculated. For the CGF of the current, the appropriate boundary condition for p at the final time is [21]

$$p(x, T) = \lambda \theta(x) \quad (15)$$

We start with a step initial density, with uniform density $\rho_{-\infty}$ to the left of the origin and $\rho_{+\infty}$ to the right of the origin, and consider two kinds of initial conditions, annealed and quenched [21, 9, 30, 31]. In the quenched case, the step initial condition is deterministic:

$$q(x, 0) = \rho_{-\infty} \theta(-x) + \rho_{+\infty} \theta(x) \quad (16)$$

In the annealed case, the initial profile is allowed to fluctuate, leading to an implicit equation for $q(x, 0)$ in terms of $p(x, 0)$:

$$p(x, 0) = \lambda \theta(x) + \theta(-x) \int_{\rho_{-\infty}}^{q(x,0)} dq \frac{2D(q)}{\sigma(q)} + \theta(x) \int_{\rho_{+\infty}}^{q(x,0)} dq \frac{2D(q)}{\sigma(q)} \quad (17)$$

2.3. Mapping the MFT equations

In this section, we show how the conductivity $\sigma(q)$ and the field p transform in the mapping from a single-file process to a mass-transport model. We use the Hamiltonian formulation [30] of the MFT equations of motion (12a) and (12b) in terms of the fields p_m and q_m for the mass-transfer model

$$H = \int dz \left(-D_m(q_m)(\partial_z q_m)(\partial_z p_m) + \frac{\sigma_m(q_m)}{2}(\partial_z p_m)^2 \right) \quad (18)$$

We transform this Hamiltonian to the single-file system by using equations (7), (8) and (11):

$$\begin{aligned} H &= \int dx \left(\frac{dz}{dx} \right) \left(-q_s^2 D_s(q_s)(\partial_x q_s^{-1})(\partial_x p_m) \left(\frac{dx}{dz} \right)^2 \right. \\ &\quad \left. + \frac{1}{2} \sigma_m \left(\frac{1}{q_s} - 1 \right) (\partial_x p_m)^2 \left(\frac{dx}{dz} \right)^2 \right) \\ &= \int dx \left(D_s(q_s)(\partial_x q_s) \left(\frac{\partial_x p_m}{q_s} \right) + \frac{q_s}{2} \sigma_m \left(\frac{1}{q_s} - 1 \right) \left(\frac{\partial_x p_m}{q_s} \right)^2 \right) \end{aligned}$$

We demand that this transformation preserves the Hamiltonian structure of the MFT equations: hence, the above Hamiltonian must take the form

$$H = \int dx \left(-D_s(q_s)(\partial_x q_s)(\partial_x p_s) + \frac{\sigma_s(q_s)}{2}(\partial_x p_s)^2 \right)$$

We deduce the following transformations rules for $(\partial_x p)$ and σ :

$$\partial_x p_s(x) = -\frac{\partial_x p_m}{q_s} = -\partial_z p_m(z) \quad (19)$$

$$\sigma_s(\rho_s) = \rho_s \sigma_m \left(\frac{1}{\rho_s} - 1 \right), \quad \text{or, } \sigma_m(\rho_m) = (1 + \rho_m) \sigma_s \left(\frac{1}{1 + \rho_m} \right) \quad (20)$$

This completes the mapping at the hydrodynamic level between a single-file system and the corresponding mass transfer process. We can verify that the hydrodynamic coefficients of SEP [30] and its corresponding ZRP are related by the transformations found above:

$$D_m(\rho_m) = \frac{1}{(1 + \rho_m)^2}, \quad \sigma(\rho_m) = \frac{2\rho_m}{1 + \rho_m} \quad (21)$$

$$D_s(\rho_s) = 1, \quad \sigma(\rho_s) = 2\rho_s(1 - \rho_s) \quad (22)$$

3. Driven tracer in SEP

We now consider a *biased* (or driven) tracer in SEP, initially located at the origin, that hops with rate r_+ to the right, and rate r_- to the left. The initial density is a step profile with density $\rho_{-\infty}$ for $x < 0$ and density $\rho_{+\infty}$ for $x > 0$. The particular dynamics of the tracer will affect the density profile in its neighborhood. We start by rederiving the expression of the density profile in a spirit close to that of [13] (see [36] for a mathematically similar problem). Then, we shall state the problem in the framework of the MFT and solve it in the high density regime.

3.1. Density profile and mean displacement

First we notice that the average density $\rho(x, t)$ of the host particles satisfies the diffusion equation

$$\frac{\partial \rho}{\partial t} = \frac{\partial^2 \rho}{\partial x^2} \quad (23)$$

In the long-time limit, fluctuations are ignored and we treat $X(t)$ as a deterministic variable. The profile $\rho(x, t)$ as seen from the tracer will adopt a stationary scaling form. This profile may be discontinuous at the position of the tracer: we denote the density profile for $x \geq X(t)$ by $\rho_R(x, t)$, and the density profile for $x \leq X(t)$ by $\rho_L(x, t)$. Similarly, ρ_+ and ρ_- will denote the limiting values of the density just to the right ($x = X(t) + 0^+$) and just to the left ($x = X(t) - 0^+$) of the tracer respectively.

The diffusion equation (23) has to be supplemented by the following boundary conditions:

$$\rho_+ \frac{dX}{dt} = - \left. \frac{\partial \rho_R(x, t)}{\partial x} \right|_{x=X^+} \quad (24)$$

$$\rho_- \frac{dX}{dt} = - \left. \frac{\partial \rho_L(x, t)}{\partial x} \right|_{x=X^-} \quad (25)$$

$$r_+(1 - \rho_+) = r_-(1 - \rho_-) \quad (26)$$

The Stefan-type boundary conditions Eq. (24) and Eq. (25), result from the conservation of the number of particles. Eq. (26) expresses the fact that the average speed of the tracer vanishes.

Hence, we must solve two diffusion equations (23) in the regions $-\infty < x < X(t)$ and $X(t) < x < +\infty$ subject to the initial condition

$$\rho(x, 0) = \rho_{-\infty} \theta(-x) + \rho_{+\infty} \theta(x) \quad (27)$$

with the boundary conditions (24) and (25). The two solutions are matched using (26).

The Stefan problem (24) admits a scaling solution of the form

$$\rho_R(x, t) = f(\xi), \quad \text{where} \quad \xi = \frac{x}{X} \quad (28)$$

With this scaling form, the heat equation and the boundary condition (24) reduce to the ordinary differential equations

$$f'' = -c_R \xi f' \quad \text{with} \quad c_R = -\frac{f'(1)}{\rho_+} \quad (29)$$

$$X \dot{X} = c_R \quad (30)$$

where the prime (the dot) denotes the derivative with respect to the scaled distance ξ (the time). Solving with the condition $f(1) = \rho_+$ leads us to

$$\rho_R(x, t) = \rho_+ \left(1 - c_R \int_1^{\frac{x}{X}} e^{c_R(1-\xi^2)/2} d\xi \right) \quad (31)$$

$$X_t = \sqrt{2c_R t} \quad (32)$$

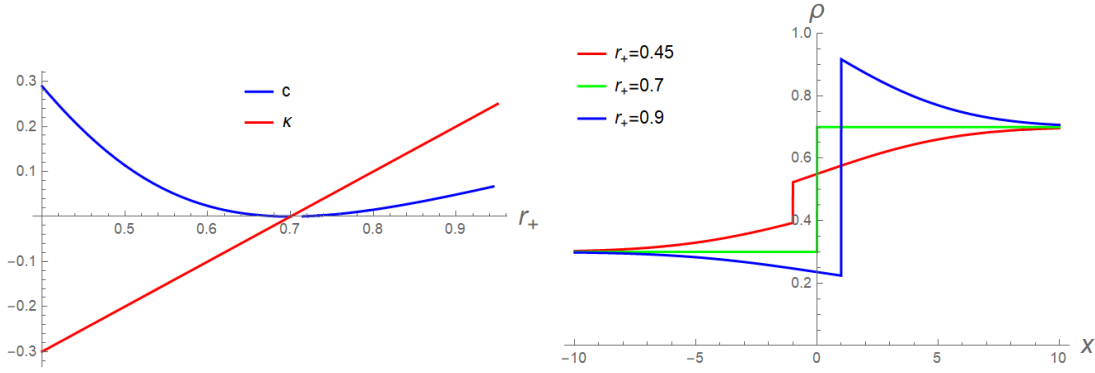


Figure 2. (a) A plot of κ and c as a function of r_+ , on the hyperplane of parameters where $r_+ + r_- = 1$, for $\rho_{+\infty} = 0.7$ and $\rho_{-\infty} = 0.3$. (b) A plot of the density profile for $t = 10$ for three values of r_+ , with the same values of other parameters as in (a). It can be seen that the particle remains stationary for $r_+ = 0.7$, and the density profile remains constant with time.

The validity of the solution requires that $c_R > 0$. Since ρ_R is monotonically decreasing, this implies that $\rho_+ > \rho_{+\infty}$. In this case, the tracer moves in the positive direction.

$$\rho_L(x, t) = \rho_- \left(1 + c_L \int_{\frac{x}{X_t}}^1 e^{c_L(1-\xi^2)/2} d\xi \right) \quad (33)$$

$$X_t = \sqrt{2c_L t} \quad (34)$$

Comparing (32) with (34) gives us $c_R = c_L$: this common value will be denoted by c . Recalling that $\rho_R(+\infty) = \rho_{+\infty}$ and $\rho_R(-\infty) = \rho_{-\infty}$, we can also deduce the relations

$$\frac{\rho_{+\infty}}{\rho_+} = 1 - c_R \int_1^{+\infty} e^{c_R(1-\xi^2)/2} d\xi = 1 - \sqrt{2\pi c} e^{c/2} \frac{1 - \operatorname{erf}(\sqrt{\frac{c}{2}})}{2} \quad (35)$$

$$\frac{\rho_{-\infty}}{\rho_-} = 1 + c_L \int_{-\infty}^1 e^{c_L(1-\xi^2)/2} d\xi = 1 + \sqrt{2\pi c} e^{c/2} \frac{1 + \operatorname{erf}(\sqrt{\frac{c}{2}})}{2} \quad (36)$$

Equations (35), (36) together with the matching condition $r_+(1 - \rho_+) = r_-(1 - \rho_-)$ (see eqn. (26)), provide us with three independent relations for the three unknowns ρ_+ , ρ_- and c . Eqn. (26) shows that the absolute values of r_+ and r_- do not matter, only the asymmetry ratio $-1 < \alpha = \frac{r_+ - r_-}{r_+ + r_-} < 1$ does. ‡

So far, we have assumed that $c > 0$, and this implies that $\rho_+ \geq \rho_{+\infty}$ and $\rho_- \leq \rho_{-\infty}$. Since eqn. (26) holds, we define the quantity

$$\kappa = r_+(1 - \rho_{+\infty}) - r_-(1 - \rho_{-\infty}) \quad (37)$$

It can be seen that $\kappa > 0$ when $c > 0$ and $\kappa = 0$ when $c = 0$. Thus, when

$$r_+(1 - \rho_{+\infty}) = r_-(1 - \rho_{-\infty}), \text{ we have } X_t = 0$$

and the tracer does not move. Now, if $\kappa < 0$, assuming for the moment that $r_+ > r_-$, the bias is not large enough to overcome the push of the density gradient, and the particle

‡ A simple procedure to analyze these equations is as follows: for any given values of $\rho_{\pm\infty}$, choose a $c > 0$ and this provides us with values of $\rho_+(c)$, $\rho_-(c)$ and $\alpha(c)$.

moves in the negative direction. To obtain the solution for the case $\kappa < 0$, we consider the mirrored system, where one exchanges r_+ and r_- , and exchanges $\rho_{+\infty}$ and $\rho_{-\infty}$. For this mirrored system, we have $\kappa > 0$ and thus can apply the method above. Let ρ_{mirror} be the density profile for this mirrored system, and c_{mirror} the value of c . The solution for $\kappa < 0$ is then

$$\begin{aligned}\rho(x, t) &= \rho_{\text{mirror}}(-x, t) \\ X_t &= -\sqrt{2c_{\text{mirror}}t}.\end{aligned}$$

Thus, we have that $X = \text{Sgn}(\kappa)\sqrt{2ct}$. Fig. 2 shows a plot of the density profile around the tracer for various values of κ .

One can look at the limit of a small asymmetry around the equilibrium state, $r_{\pm} = (1 \pm \epsilon)$, and $\rho_{+\infty} = \rho_{-\infty} = \rho$. In this limit,

$$\begin{aligned}c &= \frac{2}{\pi} \frac{(1-\rho)^2}{\rho^2} \epsilon^2 + O(\epsilon^3), \\ X_t &= \frac{2}{\sqrt{\pi}} \frac{(1-\rho)}{\rho} \epsilon \sqrt{t} + O(\epsilon^2)\end{aligned}\tag{38}$$

The value of the drift under a small bias is thus the same as the (annealed) variance without a bias, as expected from the Einstein relation [37, 28].

In the totally asymmetric case $r_- = 0$, we have $\rho_+ = 1$ irrespective of the value of r_+ . Then, in the limiting cases of small and large density, the average position of the tracer exhibits the following asymptotic behaviors:

$$X_t \simeq \sqrt{t} \times \begin{cases} \sqrt{2/\rho_{+\infty}} & \rho_{+\infty} \downarrow 0 \\ 2\pi^{-1/2}(1-\rho_{+\infty}) & \rho_{+\infty} \uparrow 1 \end{cases}\tag{39}$$

3.2. Boundary conditions at the origin

In the SEP, a biased tracer attempts a hop to the right with probability r_+ , and to the left with probability r_- . If $r_+ = r_- = 1$, the tracer is unbiased and performs the same motion as all other particles. We now consider a driven tracer in a general single-file system and define the biased dynamics carefully. If an unbiased tracer in a configuration C has a probability $p_{\text{T}}(C)$ of hopping to the right or the left, we define the driven tracer to hop to the right with rate $r_+p_{\text{T}}(C)$ and to the left with $r_-p_{\text{T}}(C)$.

In the mass-transfer picture, the movement of the tracer corresponds to biased mass transfer across the bond $[-1, 0]$. The mass transfer across this bond to the left is enhanced by a factor r_+ while transfer to the right is enhanced (or suppressed) by a factor r_- . The total displacement of the tracer is, in the ZRP picture, is minus the total current through the origin from time 0 to time t , using eqn. (6).

We will consider the MFT solutions on the two sides of the origin as separate systems on the two half-planes [38], whose solutions are related through certain boundary conditions at the origin. Assuming that the coarse-grained hydrodynamic limit remains valid, the hydrodynamic local density field during the evolution is then

given by $q(x, t)$, the solution of the MFT equations. This implies that local equilibrium holds, with the local density parameter given by $q([\ell x], t)$ where ℓ is the coarse-graining length. We also assume that the joint distribution on different sites factorizes [28, 29]. For local equilibrium to hold on both sides,

$$r_- R(\rho_{-1}) = r_+ R(\rho_0)$$

where $R(\rho)$ denotes the total rate of outward mass transfer from a site in the steady state with density ρ (we have assumed local equilibrium). Thus, in the hydrodynamic limit,

$$r_- R(q(0^-, t)) = r_+ R(q(0^+, t)), \text{ or } r_- R(q_-) = r_+ R(q_+) \quad (40)$$

where we have used the notation $g_+ \equiv g(x = 0^+)$ and $g_- \equiv g(x = 0^-)$ for the limits of a function g on either sides of the origin. The function R is related to the diffusivity as, in the presence of a uniform density gradient, the current in the continuum limit is given by

$$j = -\frac{1}{2} \partial_x R(\rho), \text{ and hence, } R'(\rho) = 2D(\rho) \quad (41)$$

where $D(\rho)$ is the diffusivity. For the ZRP, we have $R(q) = \frac{2q}{1+q}$, and the condition eqn. (40) becomes

$$r_- \frac{q_-}{1+q_-} = r_+ \frac{q_+}{1+q_+} \quad (42)$$

It is seen that this is equivalent to the SEP condition for the density profile, eqn. (26).

We now find the boundary conditions for p across the origin by considering the variation of the action. The action for a trajectory is given by [30]

$$S = \int_0^T dt \int_{-\infty}^{\infty} dx \left(p \partial_t q - \frac{\sigma(q)}{2} (\partial_x p)^2 + D(q) (\partial_x p) (\partial_x q) \right) \quad (43)$$

To derive the boundary conditions on p at the origin, we consider the variation of the action with respect to q and p . (See the [Appendix A](#) for the details of the derivation.) First, we consider the variation with respect to q , which gives boundary conditions relating the gradient of p on the two sides of the origin:

$$r_- (\partial_x p)_+ = r_+ (\partial_x p)_- \quad (44)$$

Similarly, we can consider the variation of the action with respect to p . This gives boundary conditions that relate p on the two sides of the origin,

$$p_+ = p_- \quad (45)$$

Eqns. (40), (44) and (45) complete the description of boundary conditions at the origin for a biased particle. It can be seen that the values of r_+ and r_- come into the boundary conditions only upto an overall multiplicative constant, and hence only the value of $\frac{r_+}{r_+ + r_-}$ matters to the dynamics.

Since the current at the origin is related to the displacement of the tracer, we have

$$\frac{dX}{dt} = -j_m|_{x=0^+} = -j_m|_{x=0^-} \quad (46)$$

Eqn. (42) becomes, in the SEP MFT,

$$r_+(1 - q_s)|_{x=X^+} = r_-(1 - q_s)|_{x=X^-} \quad (47)$$

The two equations above are the MFT generalization of the conditions in eqns. (24), (25) and (26). Based on these MFT equations, we propose the following fluctuating hydrodynamic equations to model the tracer hydrodynamics. In the bulk on either side of the tracer we have the equations

$$\partial_t \rho_s = -\partial_x j_s, \quad (48)$$

$$j_s = -D(\rho_s)\partial_x \rho_s + \sqrt{\sigma_s(\rho_s)}\eta \quad (49)$$

where η is a noise uncorrelated in space and time. These bulk equations are supplemented by the boundary conditions at the tracer:

$$\frac{dX}{dt} = \left(\frac{1}{\rho_s} j_s \right) \Big|_{x=X^+} = \left(\frac{1}{\rho_s} j_s \right) \Big|_{x=X^-} \quad (50)$$

$$r_+(1 - \rho_s)_+ = r_-(1 - \rho_s)_- \quad (51)$$

where for the first equation we have used eqns. (10) and (46).

4. Fluctuations of the driven tracer in the high density limit

We now consider the low-density limit in the ZRP, which corresponds to the high-density limit of the SEP. In this limit, the hydrodynamic coefficients for the ZRP become

$$D(q) = 1 + O(q), \quad \sigma(q) = 2q + O(q^2) \quad (52)$$

Away from the tracer particle, the bulk MFT equations for the ZRP hold,

$$\partial_t q = \partial_x ((\partial_x q) - 2q(\partial_x p)) \quad (53a)$$

$$\partial_t p = -\partial_x^2 p - (\partial_x p)^2 \quad (53b)$$

The Cole-Hopf transformation

$$Q = qe^{-p}, \quad P = e^p \quad (54)$$

simplifies the E-L equations into pure diffusion equations

$$\partial_t Q = \partial_x^2 Q, \quad \partial_t P = -\partial_x^2 P \quad (55)$$

In the ZRP, in the high-density limit, the SEP initial condition (27), the initial condition for the average density becomes

$$\rho_m(x, 0) = (1 - \rho_{+\infty})\theta(x) + (1 - \rho_{-\infty})\theta(-x) + O((1 - \rho)^2) \quad (56)$$

The boundary condition on $p(x, T)$, eqn. (15) becomes

$$P(x, T) = 1 + (e^\lambda - 1)\theta(x) \quad (57)$$

The quenched initial condition (16) gives

$$Q(x, 0) = \frac{1}{P(x, 0)} ((1 - \rho_{-\infty})\theta(-x) + (1 - \rho_{+\infty})\theta(x)) \quad (58)$$

For the annealed initial condition, we have, from (17) with $D(q) = 1$ and $\sigma(q) = 2q$,

$$q(x, 0) = (1 - \rho_{-\infty})e^{p(x,0)}\theta(-x) + (1 - \rho_{+\infty})e^{p(x,0)-\lambda}\theta(x), \text{ giving,} \quad (59)$$

$$Q(x, 0) = (1 - \rho_{-\infty})\theta(-x) + (1 - \rho_{+\infty})e^{-\lambda}\theta(x). \quad (60)$$

4.1. Analytic solution for $P(x, t)$

$P(x, t)$ obeys the anti-diffusion equation

$$\partial_t P = -\partial_x^2 P \quad (61)$$

with initial condition

$$P(x, T) = 1 + (e^\lambda - 1)\theta(x)$$

and boundary conditions

$$P(x, t) \rightarrow e^\lambda \text{ as } x \rightarrow \infty,$$

$$P(x, t) \rightarrow 1 \text{ as } x \rightarrow -\infty$$

The general solution is thus

$$P(x, t) = \begin{cases} e^\lambda + A \left(1 - \operatorname{erf} \left(\frac{x}{\sqrt{4(T-t)}} \right) \right) & \text{for } x > 0 \\ 1 + B \left(1 + \operatorname{erf} \left(\frac{x}{\sqrt{4(T-t)}} \right) \right) & \text{for } x < 0 \end{cases} \quad (62)$$

where A and B are constants to be determined from the boundary conditions. We now use the two conditions (44) and (45)

$$P_+ = P_-, \text{ and } r_-(\partial_x P)_+ = r_+(\partial_x P)_-$$

to solve for A and B . This gives,

$$A = \frac{r_+}{r_+ + r_-}(1 - e^\lambda), \text{ and } B = \frac{r_-}{r_+ + r_-}(e^\lambda - 1)$$

Thus, we have

$$P(x, t) = \begin{cases} e^\lambda + \frac{r_+}{r_+ + r_-}(1 - e^\lambda)\operatorname{erfc} \left(\frac{x}{\sqrt{4(T-t)}} \right) & \text{for } x > 0 \\ 1 + \frac{r_-}{r_+ + r_-}(e^\lambda - 1)\operatorname{erfc} \left(\frac{|x|}{\sqrt{4(T-t)}} \right) & \text{for } x < 0 \end{cases} \quad (63)$$

We want to determine the cumulant generating function (CGF) of the position of the tagged particle after time T ,

$$\mu^p(\lambda) = \log \langle e^{\lambda X_T} \rangle \quad (64)$$

As the position of the tagged particle in the SEP is related to the current in the ZRP through (6), we have the relation

$$\mu^p(\lambda) = \log \langle e^{\lambda X_T} \rangle = \log \langle e^{-\lambda J(T)} \rangle = \mu(-\lambda) \quad (65)$$

where $\mu(\lambda)$ is the CGF of the current in the ZRP, defined in (13). Now, using (14) we can calculate $\mu(\lambda)$ through the MFT solution,

$$\begin{aligned} \mu'(\lambda) &= \int_0^\infty dx (q(x, T) - q(x, 0)) \\ &= \int_0^\infty dx (Q(x, T)P(x, T) - Q(x, 0)P(x, 0)) \end{aligned} \quad (66)$$

$Q(x, t)$ evolves according to a pure diffusion equation with the boundary condition at the origin, using eqn. (42),

$$r_+ Q(0^+, t) = r_- Q(0^-, t) \quad (67)$$

Conservation of the current of q across the origin gives

$$(\partial_x Q)_- = (\partial_x Q)_+ \quad (68)$$

Consider a general initial condition

$$Q(x, 0) = Q_1(x)\Theta(x) + Q_2(x)\Theta(-x) \quad (69)$$

The general solution for $x > 0$ satisfying the boundary conditions is (see [Appendix B](#) for details)

$$\begin{aligned} Q(x, t) &= \int_0^\infty \frac{dy}{\sqrt{4\pi t}} \left[Q_1(y) \left(e^{-\frac{(x-y)^2}{4t}} - \frac{r_+ - r_-}{r_+ + r_-} e^{-\frac{(x+y)^2}{4t}} \right) \right. \\ &\quad \left. + \frac{2r_-}{r_+ + r_-} Q_2(y) e^{-\frac{(x+y)^2}{4t}} \right] \end{aligned}$$

Inserting the solutions for Q and P into eqn. (66), and performing the integral over x , we get

$$\begin{aligned} \mu'(\lambda) &= - \int_0^\infty dy Q_1(y) \left(e^\lambda + \frac{r_+}{r_+ + r_-} (1 - e^\lambda) \operatorname{erfc} \left(\frac{y}{\sqrt{4T}} \right) \right) \\ &\quad + \int_0^\infty dy Q_1(y) e^\lambda \left(1 - \frac{r_+}{r_+ + r_-} \operatorname{erfc} \left(\frac{y}{\sqrt{4T}} \right) \right) \\ &\quad + \int_0^\infty dy Q_2(y) e^\lambda \frac{r_-}{r_+ + r_-} \operatorname{erfc} \left(\frac{y}{\sqrt{4T}} \right) \\ &= \int_0^\infty dy \left(-\frac{r_+}{r_+ + r_-} Q_1(y) \operatorname{erfc} \left(\frac{y}{\sqrt{4T}} \right) + \frac{r_-}{r_+ + r_-} Q_2(y) e^\lambda \operatorname{erfc} \left(\frac{y}{\sqrt{4T}} \right) \right) \end{aligned} \quad (70)$$

4.2. Cumulants in the Annealed Case

For the annealed case, inserting the initial condition (60) into eqn. (70),

$$\begin{aligned}\mu'_a(\lambda) &= \frac{\sqrt{4T}}{r_+ + r_-} \left(-(1 - \rho_{+\infty})r_+e^{-\lambda} + (1 - \rho_{-\infty})r_-e^\lambda \right) \int_0^\infty dy \operatorname{erfc}(y) \\ &= \sqrt{\frac{4T}{\pi}} \frac{1}{r_+ + r_-} \left(-(1 - \rho_{+\infty})r_+e^{-\lambda} + (1 - \rho_{-\infty})r_-e^\lambda \right)\end{aligned}\quad (71)$$

We thus have, using the condition that $\mu_a(0) = 0$,

$$\frac{\mu_a^p(\lambda)}{\sqrt{4T}} = \frac{\mu_a(-\lambda)}{\sqrt{4T}} = \frac{(1 - \rho_{+\infty})r_+(e^\lambda - 1) + (1 - \rho_{-\infty})r_-(e^{-\lambda} - 1)}{\sqrt{\pi}(r_+ + r_-)} + O((1 - \rho)^2) \quad (72)$$

where we have made explicit that the results here are derived in the high-density limit of the SEP.

4.3. Cumulants in the Quenched Case

For the quenched case, we have the initial condition (58), which gives,

$$\mu'_q(\lambda) = \int_0^\infty dy \left(-\frac{(1 - \rho_{+\infty})\frac{r_+}{r_+ + r_-}e^{-\lambda}\operatorname{erfc}\left(\frac{y}{\sqrt{4T}}\right)}{1 + \frac{r_+}{r_+ + r_-}(e^{-\lambda} - 1)\operatorname{erfc}\left(\frac{y}{\sqrt{4T}}\right)} + \frac{(1 - \rho_{-\infty})\frac{r_-}{r_+ + r_-}e^\lambda\operatorname{erfc}\left(\frac{y}{\sqrt{4T}}\right)}{1 + \frac{r_-}{r_+ + r_-}(e^\lambda - 1)\operatorname{erfc}\left(\frac{y}{\sqrt{4T}}\right)} \right)$$

Which then gives, for the CGF,

$$\begin{aligned}\frac{\mu_q^p(\lambda)}{\sqrt{4T}} = \frac{\mu_q(-\lambda)}{\sqrt{4T}} &= \int_0^\infty dy \left[(1 - \rho_{+\infty}) \log \left(1 + \frac{r_+}{r_+ + r_-}(e^\lambda - 1)\operatorname{erfc}(y) \right) \right. \\ &\quad \left. + (1 - \rho_{-\infty}) \log \left(1 + \frac{r_-}{r_+ + r_-}(e^{-\lambda} - 1)\operatorname{erfc}(y) \right) \right] + O((1 - \rho)^2)\end{aligned}\quad (73)$$

where we have made the high-density limit explicit. Equations (72) and (73) are in agreement with the results of [15, 26], derived using a microscopic approach.

4.4. The variance for a general initial condition

Following Banerjee et al [34], we now consider more general initial conditions described by a generalized susceptibility, such that the log-probability of a small density variation in the initial ensemble is given by

$$F(\{q(x, 0)\}) \approx \frac{1}{2} \int_{-\infty}^0 dx \frac{(q(x, 0) - (1 - \rho_{-\infty}))^2}{\alpha_{\text{ic}}(1 - \rho_{-\infty})} + \frac{1}{2} \int_0^\infty dx \frac{(q(x, 0) - (1 - \rho_{+\infty}))^2}{\alpha_{\text{ic}}(1 - \rho_{+\infty})} \quad (74)$$

where we have kept terms only to quadratic order in the variation. The quantity α_{ic} defines a generalized susceptibility, and is related to the Fano factor [34]. The generalized susceptibility α_{ic} describes the amount of fluctuations in the initial ensemble. For the

quenched or hyperuniform [39, 40] initial conditions, $\alpha_{\text{ic}} = 0$, while for annealed initial conditions, because local equilibrium is a Poisson state, $\alpha_{\text{ic}} = 1$.

We analyze the dependence of the variance of the biased tracer position on α_{ic} . This involves terms to second order in the CGF $\mu(\lambda)$, and hence to first order in $q(x, t)$. For an ensemble of initial conditions described by the log-probability function F , the initial condition for q is given implicitly by [21]

$$p(x, 0) = \lambda\theta(x) + \frac{\delta F}{\delta q(x, 0)}, \quad (75)$$

which gives

$$q(x, 0) \approx \theta(-x)(1 - \rho_{-\infty})(1 + \alpha_{\text{ic}}p(x, 0)) + \theta(x)(1 - \rho_{+\infty})(1 + \alpha_{\text{ic}}(p(x, 0) - \lambda)) \quad (76)$$

to $O(\lambda^2)$ and $O((1 - \rho)^2)$. For $\alpha_{\text{ic}} = 0$, we have the quenched initial conditions, while the case $\alpha_{\text{ic}} = 1$ is equivalent to eqn. (59) first order in λ . Since $q(x, t)$ is a linear function of α_{ic} , and the MFT equations (12a) and (12b) are linear to first order in λ [31], it is expected that $\mu'(\lambda)$ to first order for general α_{ic} will be a linear combination of the quenched and annealed answers.

Using the Cole-Hopf transformation and eqn. (63), and keeping terms only to $O(\lambda)$ and in the high-density limit,

$$\begin{aligned} Q_1(x) &= (1 - \rho_{+\infty}) - \lambda (1 - \rho_{+\infty})(1 - \alpha_{\text{ic}}) \left(1 - \frac{r_+}{r_+ + r_-} \text{Erfc} \left(\frac{y}{\sqrt{4T}} \right) \right) \\ Q_2(x) &= (1 - \rho_{-\infty}) - \lambda \frac{r_-}{r_+ + r_-} (1 - \rho_{-\infty})(1 - \alpha_{\text{ic}}) \text{Erfc} \left(\frac{y}{\sqrt{4T}} \right) \end{aligned}$$

Inserting into eqn. (70), we have

$$\begin{aligned} \mu'(\lambda) &= \frac{\sqrt{4T}}{\sqrt{\pi}(r_+ + r_-)} \left\{ (1 - \rho_{-\infty})r_- - (1 - \rho_{+\infty})r_+ \right. \\ &\quad \left. + \lambda \left[(1 - \rho_{+\infty})r_+ \left(1 - (\sqrt{2} - 2) (\alpha_{\text{ic}} - 1) \frac{r_+}{r_+ + r_-} \right) \right. \right. \\ &\quad \left. \left. + (1 - \rho_{-\infty})r_- \left(1 - (\sqrt{2} - 2) (\alpha_{\text{ic}} - 1) \frac{r_-}{r_+ + r_-} \right) \right] \right\} \\ &= J_{\text{quenched}} + \alpha_{\text{ic}} (J_{\text{annealed}} - J_{\text{quenched}}) + O(\lambda^2) + O((1 - \rho)^2) \quad (77) \end{aligned}$$

The cases $\alpha_{\text{ic}} = 0$ and $\alpha_{\text{ic}} = 1$ give back the results, to $O(\lambda)$, of eqns. (73) and (72). From eqn. (77), we get that the second cumulant of the biased tracer position in the high-density limit is

$$\langle X^2 \rangle_c = \langle X^2 \rangle_{c, \text{quenched}} + \alpha_{\text{ic}} (\langle X^2 \rangle_{c, \text{annealed}} - \langle X^2 \rangle_{c, \text{quenched}}) \quad (78)$$

Thus, the dependence of the second cumulant on α_{ic} follows the same pattern for a biased tracer as that found for unbiased tracers in [34].

5. Concluding remarks

In this paper, we have investigated the problem of a biased tracer in a single-file system. Thanks to a mapping to a ZRP with a biased bond at the origin, we could write exact boundary conditions at the origin within the MFT framework, solve the high density limit, retrieve at the macroscopic scale the results of microscopic calculations [15, 26] and study a whole family of initial conditions, thus generalizing the results of [34] to biased tracers.

We emphasize that the boundary conditions derived here are valid for general single-file systems and thus open up the MFT framework for investigating biased tracers. The fluctuating hydrodynamic equations (48)- (51) could also be useful for numerical investigation as well as for perturbative calculations. We expect that this continuous approach, that takes fluctuations into account, will be useful for investigating the effect of a local defect at the global hydrodynamic scale.

While completing this manuscript, we became aware of a related work ‘Duality in single-file diffusion’ by our colleagues P. Rizkallah, A. Grabsch, P. Illien and Olivier Bénichou from Sorbonne University (arXiv 2207.07549): they also consider the mapping from a single-file to a mass-transfer process to find relations between various models and to transfer exact solutions between them. We were motivated by a different problem, the biased tracer and the mapping was introduced to rewrite a (stochastic) moving Stefan problem as a localized boundary condition.

Acknowledgements

We would like to thank Paul Krapivsky for early collaboration and helpful discussions and comments on the manuscript.

Appendix A. Boundary conditions on p at the biased particle

First we consider the variation in the MFT action S (eqn. (43)) in terms of the variation in q . We only keep the terms which are total derivatives in space (the bulk variation gives the E-L equations (12a) and (12b) and the total time-derivative terms give the boundary conditions [21]),

$$\begin{aligned} \delta S = \int_0^T dt & \left([\delta q D(q) \partial_x p]_{x=\infty} - [\delta q D(q) \partial_x p]_{x=0^+} \right. \\ & \left. + [\delta q D(q) \partial_x p]_{x=0^-} - [\delta q D(q) \partial_x p]_{x=-\infty} \right) \end{aligned} \quad (\text{A.1})$$

We now use the fact that $(\partial_x p) \rightarrow 0$ as $x \rightarrow \pm\infty$, to get

$$\begin{aligned} 0 &= \int_0^T dt \left([\delta q_+ D(q_+) \partial_x p]_+ - [\delta q_- D(q_-) \partial_x p]_- \right) \\ &= \int_0^T dt (\delta R(q_+) (\partial_x p)_+ - \delta R(q_-) (\partial_x p)_-) \end{aligned}$$

where we have used eqn. (41). Now using eqn. (40), we get that

$$r_+ \delta R(q_+) = r_- \delta R(q_-)$$

and hence,

$$\delta S = \int_0^T dt \delta R(q_+) (r_- (\partial_x p)_+ - r_+ (\partial_x p)_-) = 0$$

and hence,

$$r_- (\partial_x p)_+ = r_+ (\partial_x p)_- \quad (\text{A.2})$$

The boundary terms in the variation in p can be similarly computed to be

$$\delta S = \int_0^T dt (\delta p_+ (\sigma(q) (\partial_x p) - D(q) (\partial_x q))_+ - \delta p_- (\sigma(q) (\partial_x p) - D(q) (\partial_x q))_-)$$

Now, it is known that in the MFT, the density field q is conserved, and hence, the current flowing from the right to the origin is equal to the current flowing to the left from the origin,

$$(\sigma(q) (\partial_x p) - D(q) (\partial_x q))_+ = (\sigma(q) (\partial_x p) - D(q) (\partial_x q))_- \quad (\text{A.3})$$

For this to happen, it must be that case that δp_+ and δp_- cannot vary independently, that is,

$$\delta p_- = \delta p_+, \text{ that is, } p_+ = p_- + C \quad (\text{A.4})$$

The constant C can be fixed by looking at the right hand side of (12b), where $C \neq 0$ would lead to an unphysical delta-function-squared term. Hence,

$$p_+ = p_- \quad (\text{A.5})$$

Appendix B. General solution for $Q(x, t)$

In this Appendix we calculate a general formula for $Q(x, t) = q(x, t)e^{-p(x, t)}$ evolving according to the diffusion equation (55) and the boundary conditions

$$r_+ Q(0^+, t) = r_- Q(0^-, t) \text{ for } t > 0, \text{ and } (\partial_x Q)_+ = (\partial_x Q)_- \quad (\text{B.1})$$

The latter equation comes from the conservation of the current of q across the origin, (A.3) and using the boundary conditions (42), (44) and (45). We consider the initial condition

$$Q(x, 0) = Q_1(x)\Theta(x) + Q_2(x)\Theta(-x)$$

Since the values of Q on either side of the origin are constrained to be different, we consider a partial mirror-image solution on the two sides of the origin,

$$Q(x, 0) = \begin{cases} \int_0^\infty \frac{dy}{\sqrt{4\pi t}} \left(Q_1(y) \left(e^{-\frac{(x-y)^2}{4t}} - a e^{-\frac{(x+y)^2}{4t}} \right) + (1-a) Q_2(y) e^{-\frac{(x+y)^2}{4t}} \right) & \text{for } x > 0 \\ \int_{-\infty}^0 \frac{dy}{\sqrt{4\pi t}} \left(Q_2(y) \left(e^{-\frac{(x-y)^2}{4t}} - b e^{-\frac{(x+y)^2}{4t}} \right) + (1-b) Q_1(y) e^{-\frac{(x+y)^2}{4t}} \right) & \text{for } x < 0 \end{cases}$$

where a and b are constants determined from the boundary conditions in (B.1), which give

$$r_+(1-a) = r_-(1-b) \text{ and } a = -b,$$

Hence, we have

$$a = -b = \frac{r_+ - r_-}{r_+ + r_-} \quad (\text{B.2})$$

References

- [1] H. Spohn. *Large Scale Dynamics of Interacting Particles*. Springer, Berlin, 1991.
- [2] B. Schmittmann and R. K. P. Zia. Statistical mechanics of driven diffusive systems. In C. Domb and J. L. Lebowitz, editors, *Phase Transitions and Critical Phenomena*, volume 17, pages 3–214. Academic Press, London, 1995.
- [3] T. M. Liggett. *Stochastic Interacting Systems: Contact, Voter, and Exclusion Processes*. Springer, Berlin, 1999.
- [4] C. Kipnis and C. Landim. *Scaling Limits of Interacting Particle Systems*. Springer, Berlin, 1999.
- [5] T. Chou, K. K. Mallick, and R. K. P. Zia. Non-equilibrium statistical mechanics: from a paradigmatic model to biological transport. *Rep. Progr. Phys.*, 74(11):116601, oct 2011.
- [6] C. T. MacDonald, J. H. Gibbs, and A. C. Pipkin. Kinetics of biopolymerization on nucleic acid templates. *Biopolymers*, 6:1–25, 1968.
- [7] C. T. MacDonald and J. H. Gibbs. Concerning the kinetics of polypeptide synthesis on polyribosomes. *Biopolymers*, 7:707–725, 1969.
- [8] G. M. Schütz. Exactly solvable models for many-body systems far from equilibrium. In C. Domb and J. L. Lebowitz, editors, *Phase Transitions and Critical Phenomena*, volume 19, pages 1–251. Academic Press, London, 2001.
- [9] B. Derrida. Non-equilibrium steady states: fluctuations and large deviations of the density and of the current. *J. Stat. Mech.*, P07023, 2007.
- [10] C. Kipnis, S. Olla, and S. R. S. Varadhan. Hydrodynamics and large deviations for simple exclusion processes. *Commun. Pure Appl. Math.*, 42:115–137, 1989.
- [11] H. Touchette. The large deviation approach to statistical mechanics. *Phys. Reports*, 478:1–69, 2009.
- [12] L. Bertini, A. De Sole, D. Gabrielli, G. Jona-Lasinio, and C. Landim. Fluctuations in stationary non-equilibrium states of irreversible processes. *Phys. Rev. Lett.*, 87:040601, 2001.
- [13] SF Burlatsky, GS Oshanin, AV Mogutov, and M Moreau. Directed walk in a one-dimensional lattice gas. *Physics Letters A*, 166(3-4):230–234, 1992.
- [14] G Oshanin, J De Coninck, M Moreau, and SF Burlatsky. Phase boundary dynamics in a one-dimensional non-equilibrium lattice gas. *arXiv preprint cond-mat/9910243*, 1999.
- [15] P Illien, O Bénichou, C Mejía-Monasterio, G Oshanin, and R Voituriez. Active transport in dense diffusive single-file systems. *Physical review letters*, 111(3):038102, 2013.

- [16] O Bénichou, P Illien, G Oshanin, A Sarracino, and R Voituriez. Nonlinear response and emerging nonequilibrium microstructures for biased diffusion in confined crowded environments. *Physical Review E*, 93(3):032128, 2016.
- [17] Theodore E Harris. Diffusion with “collisions” between particles. *Journal of Applied Probability*, 2(2):323–338, 1965.
- [18] Richard Arratia. The motion of a tagged particle in the simple symmetric exclusion system on z . *The Annals of Probability*, 11(2):362–373, 1983.
- [19] Binhua Lin, Mati Meron, Bianxiao Cui, Stuart A Rice, and Haim Diamant. From random walk to single-file diffusion. *Physical review letters*, 94(21):216001, 2005.
- [20] R Rajesh and Satya N Majumdar. Exact tagged particle correlations in the random average process. *Physical Review E*, 64(3):036103, 2001.
- [21] Bernard Derrida and Antoine Gerschenfeld. Current fluctuations in one dimensional diffusive systems with a step initial density profile. *Journal of Statistical Physics*, 137(5):978–1000, 2009.
- [22] PL Krapivsky, Kirone Mallick, and Tridib Sadhu. Large deviations in single-file diffusion. *Physical review letters*, 113(7):078101, 2014.
- [23] Paul L Krapivsky, Kirone Mallick, and Tridib Sadhu. Tagged particle in single-file diffusion. *Journal of Statistical Physics*, 160(4):885–925, 2015.
- [24] Chaitra Hegde, Sanjib Sabhapandit, and Abhishek Dhar. Universal large deviations for the tagged particle in single-file motion. *Physical review letters*, 113(12):120601, 2014.
- [25] Takashi Imamura, Kirone Mallick, and Tomohiro Sasamoto. Large deviations of a tracer in the symmetric exclusion process. *Physical Review Letters*, 118(16):160601, 2017.
- [26] Alexis Poncet, Olivier Bénichou, and Pierre Illien. Cumulant generating functions of a tracer in quenched dense symmetric exclusion processes. *Physical Review E*, 103(4):L040103, 2021.
- [27] Alexis Poncet, Aurélien Grabsch, Olivier Bénichou, and Pierre Illien. Exact time dependence of the cumulants of a tracer position in a dense lattice gas. *Physical Review E*, 105:054139, 2022.
- [28] C Landim, S Olla, and SB Volchan. Driven tracer particle in one dimensional symmetric simple exclusion. *Communications in mathematical physics*, 192(2):287–307, 1998.
- [29] Cláudio Landim and Sérgio B Volchan. Equilibrium fluctuations for a driven tracer particle dynamics. *Stochastic processes and their applications*, 85(1):139–158, 2000.
- [30] L. Bertini, A. De Sole, D. Gabrielli, G. Jona-Lasinio, and C. Landim. Macroscopic fluctuation theory. *Rev. Mod. Phys.*, 87:593–636, 2015.
- [31] PL Krapivsky and Baruch Meerson. Fluctuations of current in nonstationary diffusive lattice gases. *Physical Review E*, 86(3):031106, 2012.
- [32] Martin R Evans, Satya N Majumdar, and Royce KP Zia. Factorized steady states in mass transport models. *Journal of Physics A: Mathematical and General*, 37(25):L275, 2004.
- [33] Martin R Evans and Tom Hanney. Nonequilibrium statistical mechanics of the zero-range process and related models. *Journal of Physics A: Mathematical and General*, 38(19):R195, 2005.
- [34] Tirthankar Banerjee, Robert L Jack, and Michael E Cates. Role of initial conditions in $1d$ diffusive systems: compressibility, hyperuniformity and long-term memory. *arXiv preprint arXiv:2206.08739*, 2022.
- [35] Eldad Bettelheim, Naftali R Smith, and Baruch Meerson. Inverse scattering method solves the problem of full statistics of nonstationary heat transfer in the kipnis-marchioro-presutti model. *Physical Review Letters*, 128(13):130602, 2022.
- [36] Tibor Antal, PL Krapivsky, and S Redner. Shepherd model for knot-limited polymer ejection from a capsid. *Journal of theoretical biology*, 261(3):488–493, 2009.
- [37] Pablo A Ferrari, Sheldon Goldstein, and Joel L Lebowitz. Diffusion, mobility and the einstein relation. In *Statistical physics and dynamical systems*, pages 405–441. Springer, 1985.
- [38] Baruch Meerson and S Redner. Large fluctuations in diffusion-controlled absorption. *Journal of Statistical Mechanics: Theory and Experiment*, 2014(8):P08008, 2014.
- [39] Salvatore Torquato and Frank H Stillinger. Local density fluctuations, hyperuniformity, and order metrics. *Physical Review E*, 68(4):041113, 2003.

- [40] Rahul Dandekar. Exact hyperuniformity exponents and entropy cusps in models of active-absorbing transition. *Europhysics Letters*, 132(1):10008, 2020.